PFC/JA-80-25

TEARING-MODE STABILITY PROPERTIES OF A DIFFUSE ANISOTROPIC FIELD-REVERSED ION LAYER AT MARGINAL STABILITY

James Chen
Ronald C. Davidson

12/3/80

TEARING-MODE STABILITY PROPERTIES OF A DIFFUSE ANISOTROPIC FIELD-REVERSED ION LAYER AT MARGINAL STABILITY

James Chen and Ronald C. Davidson
Plasma Fusion Center
Massachusetts Institute of Technology, Cambridge, Mass., 02139

Stability properties are investigated for purely growing ($\mathrm{Re}\omega = 0$) tearing modes at marginal stability ($\mathrm{Im}\omega = 0$) for a rotating, non-relativistic cylindrically symmetric ion layer immersed in an axial magnetic field $B_z^0(r)\hat{e}_z = [B_0 + B_z^s(r)]\hat{e}_z$. The analysis is carried out within the framework of a Vlasov-fluid model in which the electrons are described as a macroscopic, cold fluid, and the layer ions are described by the Vlasov equation. Tearing-mode stability properties are calculated numerically for azimuthally symmetric perturbations about an anisotropic ion layer equilibrium described by $f_i^0 = \text{const} \times \exp[-(H_\perp + \omega_\theta P_\theta)/T_\perp - H_{||}/T_{||}]$. Here, $H_\perp$ is the perpendicular energy, $H_{||}$ is the parallel energy, P_θ is the canonical angular momentum, $T_\perp = \text{const.}$ and $T_{||} = \text{const.}$ are the temperatures, $-\omega_\theta = \text{const}$ is the angular velocity of mean rotation, and the density profile is $n(r) = n_0 \mathrm{sech}^2(r^2/2\delta^2 - r_0^2/2\delta^2)$, where $\delta^4 = 2c^2T_\perp/(m_i\omega_\theta^2\omega_{pi}^2)$ and $\omega_{pi}^2 = 4\pi n_0 e^2/m_i$. The marginal stability eigenvalue equation for the perturbation amplitude $\hat{A}_\theta(r)$ has the form of a Schroedinger equation, with "energy" eigenvalue $k_z^2\delta^2$ and effective potential $V(r)$. This equation is solved numerically for $\hat{A}_\theta(r)$ and the normalized axial wavenumber at marginal stability (denoted by $k_0^2\delta^2$) as a function of temperature anisotropy $T_{||}/T_\perp$, normalized layer radius r_0/δ, and magnetic field depression $\beta_i^{-1/2}[B_0 - B_z^0(r = 0)]/B_0$, where $\beta_i = 8\pi n_0 T_\perp/B_0^2$. It is found that the range of unstable wavenumbers decreases as $T_{||}/T_\perp$ is increased, and numerical estimates are made of the anisotropy required for complete stabilization.

I. INTRODUCTION

There is considerable interest in the basic equilibrium, stability and transport properties of intense ion beams in a background plasma. As a result of recent technological advances in the generation of intense ion beams, such beams have a variety of possible applications, including (a) the production of field-reversed configurations for magnetic fusion applications,[1-9] (b) applications to light ion[10-14] and heavy ion[15,16] fusion, and (c) the development of novel techniques for focussing intense ion beams.[17] In this paper, we investigate stability properties for purely growing ($Re\omega = 0$) tearing modes at marginal stability ($Im\omega = 0$) in a rotating, nonrelativistic, cylindrically symmetric ion layer immersed in an axial magnetic field $B_z^0(r)\hat{e}_z = [B_0 + B_z^s(r)]\hat{e}_z$. The analysis is carried out within the framework of a hybrid (Vlasov-fluid) model[18] in which the electrons are described as a macroscopic, cold fluid, and the layer ions are described by the Vlasov equation (Sec. II). Unlike previous detailed analyses[9] of the tearing-mode instability, no a priori assumption is made that the radial thickness (δ) of the layer is small in comparison with the mean radius (r_0). Moreover, the numerical analysis is carried out with full cylindrical effects, and not within the context of the slab approximation.[7]

Tearing-mode stability properties are calculated in Sec. III for the specific choice of ion distribution function [Eq. (28)] corresponding to the anisotropic equilibrium

$$f_i^0(H_\perp + \omega_\theta P_\theta, H_{||}) = \frac{n_0}{(2\pi T_\perp/m_i)} \frac{1}{(2\pi T_{||}/m_i)^{1/2}}$$

$$\times \exp[-(H_\perp + \omega_\theta P_\theta)/T_\perp - H_{||}/T_{||}] ,$$

where $H_\perp = (m_i/2)(v_r^2 + v_\theta^2)$ is the perpendicular energy, $H_{||} = (m_i/2)v_z^2$ is the parallel energy, P_θ is the canonical angular momentum, $T_\perp$ = const. is the perpendicular temperature, $T_{||}$ = const. is the parallel temperature, n_0 = const. is the maximum density, and $-\omega_\theta$ = const. is the angular velocity of mean rotation. The density profile corresponding to Eq. (28) is [Eq. (29)]

$$n(r) = n_0 \mathrm{sech}^2\left(\frac{r^2 - r_0^2}{2\delta^2}\right),$$

where r_0^2 = const., $\delta^4 = 2c^2T_\perp/(m_i\omega_\theta^2\omega_{pi}^2)$ and $\omega_{pi}^2 = 4\pi n_0 e^2/m_i$. In the present analysis, we assume that the net current carried by the background electrons is equal to zero, so that the magnetic self field $B_z^s(r)$ is generated entirely by the mean rotational motion of the ions.

The stability analysis in Secs. II and III assumes azimuthally symmetric perturbations ($\partial/\partial\theta = 0$) of the form $\delta\psi(\underset{\sim}{x},t) = \hat{\psi}(r)\exp(ik_z z - i\omega t)$, and the exact $\omega = 0$ eigenvalue equation (18) is derived for the general class of anisotropic rigid-rotor ion equilibria $f_i^0(H_\perp + \omega_\theta P_\theta, H_{||})$. For the specific choice of equilibrium ion distribution function in Eq. (28), the eigenvalue equation (18) is investigated numerically in Sec. III for two cases: (a) isotropic equilibrium with $T_\perp = T_{||}$ and $\partial f_i^0/\partial H_\perp = \partial f_i^0/\partial H_{||}$, and (b) anisotropic equilibrium with $T_{||} > T_\perp$ and $\partial f_i^0/\partial H_\perp \neq \partial f_i^0/\partial H_{||}$.

In the isotropic case (Secs. II.B and III.B), the general eigenvalue equation (18) reduces exactly to Eq. (35) for the choice of equilibrium distribution function in Eq. (28). Moreover, Eq. (35) has the form of a Schroedinger equation for the perturbation amplitude $\hat{A}_\theta(r)$, with "energy" eigenvalue $k^2 = k_z^2\delta^2$ and effective potential [Eq. (36)]

$$V(R) = \frac{1}{R^2} - 2R^2\mathrm{sech}^2\left(\frac{R^2 - R_0^2}{2}\right),$$

where $R = r/\delta$ and $R_0 = r_0/\delta$. In Sec. III.B, Eq. (35) is solved numerically for both the eigenfunction $\hat{A}_\theta(R)$ and the eigenvalue (denoted by $k_0^2\delta^2$) as a function of normalized layer radius r_0/δ and normalized magnetic field depression $\beta_i^{-1/2}[B_0 - B_z^0(r = 0)]/B_0$, where $\beta_i = 8\pi n_0 T_\perp/B_0^2$. This procedure determines the critical axial wavenumber k_0 corresponding to marginal stability ($\mathrm{Im}\omega = 0$). In particular, purely growing (and purely damped) solutions exist for axial wavenumber k_z in the range $0 < k_z^2 < k_0^2$.[9] On the other hand, $\mathrm{Im}\omega = 0$ for $k_z^2 \geq k_0^2$, and $\mathrm{Re}\omega$ is generally non-zero. For $r_0^2/\delta^2 > 1$, the numerical analysis shows that $k_0^2\delta^2$ can be approximated by [Eq. (39)],

$$k_0^2\delta^2 = r_0^2/\delta^2 \ ,$$

to a high degree of accuracy.

In the anisotropic case (Secs. II.C and III.C), the eigenvalue equation (18) can be approximated by Eq. (40) in circumstances where the ion layer is thin ($r_0/\delta \gg 1$) and the equilibrium distribution function is specified by Eq. (28). As in the isotropic case, Eq. (40) has the form of a Schroedinger equation with effective potential [Eq. (42)]

$$V(R) = \frac{1}{R^2} - 2R^2\,\mathrm{sech}^2\left(\frac{R^2 - R_0^2}{2}\right) + \left(1 - \frac{T_\perp}{T_\parallel}\right) \times \left(\frac{\omega_{pi}^2\delta^2}{c^2} + 2R^2\right)\mathrm{sech}^2\left(\frac{R^2 - R_0^2}{2}\right) .$$

From Eq. (42), it is evident that temperature anisotropy with $T_\parallel > T_\perp$ has the effect of <u>reducing</u> the depth of the potential well, and thereby reducing the value of $k_0^2\delta^2$ corresponding to marginal stability. Equation (40) is solved numerically in Sec. III.C for a broad range of system parameters and marginal stability properties are investigated in detail as a function of $\omega_\theta/\omega_{ci}$, $T_\parallel/T_\perp$ and r_0^2/δ^2.

II. THEORETICAL MODEL

A. General Eigenvalue Equation at Marginal Stability

The present analysis is carried out for perturbation frequencies ω satisfying $|\omega| \lesssim \omega_{ci}$, where $\omega_{ci} = eB_0/m_i c$ is the ion cyclotron frequency associated with the externally applied field B_0. In this regard, charge neutrality is assumed to first order, and the displacement current is neglected in the $\nabla \times \delta\underset{\sim}{B}$ Maxwell equation. It is also assumed that the equilibrium radial electric field is equal to zero ($E_r^0 = 0$), which is consistent with local equilibrium charge neutrality, $n_e^0(r) = n_i^0(r) \equiv n(r)$. To further simplify the analysis, we assume that all of the equilibrium current is carried by the layer ions, and that the mean equilibrium flow velocity of the electrons is equal to zero ($\underset{\sim}{V}_e^0 = 0$). Moreover, under typical experimental conditions, the thermal ion gyroradius can be comparable in size to the layer radius. Thus, in the present analysis, the layer ions are described by the Vlasov equation, and the electrons are described as a macroscopic cold fluid. Such a hybrid model[18] has proved useful in describing the equilibrium and stability properties for a variety of field-reversed configurations[9] and linear fusion systems.[19]

In the stability analysis, we consider azimuthally symmetric perturbations characterized by $\partial/\partial\theta = 0$. Using the method of characteristics, the linearized Vlasov equation for the ions can be integrated to give

$$\delta f_i(\underset{\sim}{x},\underset{\sim}{v},t) = -\frac{e}{m_i}\int_{-\infty}^{t} dt' \left(\delta\underset{\sim}{E}(\underset{\sim}{x}',t') + \frac{\underset{\sim}{v}' \times \delta\underset{\sim}{B}(\underset{\sim}{x}',t')}{c}\right) \cdot \frac{\partial}{\partial \underset{\sim}{v}'} f_i^0(\underset{\sim}{x}',\underset{\sim}{v}') \ , \tag{1}$$

where the particle trajectories $(\underset{\sim}{x}', \underset{\sim}{v}')$ satisfy $d\underset{\sim}{x}'/dt' = \underset{\sim}{v}'$ and $d\underset{\sim}{v}'/dt' = e\underset{\sim}{v}' \times B_z^0(r')\hat{\underset{\sim}{e}}_z/m_i c$, with initial conditions $\underset{\sim}{x}'(t' = t) = \underset{\sim}{x}$ and $\underset{\sim}{v}'(t' = t) = \underset{\sim}{v}$. In Eq. (1),

$$f_i^0(H_\perp + \omega_\theta P_\theta, H_{||}) = F(H_\perp + \omega_\theta P_\theta)G(H_{||}) ,$$

is a function of the single-particle constants of the motion $(H_\perp, P_\theta, H_{||})$ in the equilibrium field configuration. Here, $H_\perp = (m_i/2)(v_r^2 + v_\theta^2)$ is the perpendicular kinetic energy, $H_{||} = (m_i/2)v_z^2$ is the parallel kinetic energy, $P_\theta = m_i r v_\theta + (e/c)rA_\theta^0(r)$ is the canonical angular momentum, and $G(H_z)$ is normalized according to $\int_{-\infty}^{\infty} dv_z G(H_z) = 1$, without loss of generality. Moreover, $+e$ is the ion charge, m_i is the ion mass, $-\omega_\theta = r^{-1}(\int d^3v\ v_\theta f_i^0)/(\int d^3v\ f_i^0) = \text{const.}$ is the mean angular velocity of the layer ions, and the equilibrium axial magnetic field $B_z^0(r)$ is related to the equilibrium vector potential $A_\theta^0(r)$ by $B_z^0(r) = r^{-1}(\partial/\partial r)(rA_\theta^0)$. The axial magnetic field $B_z^0(r)$ is determined self-consistently from $\partial B_z^0/\partial r = (4\pi e/c)\omega_\theta r n(r)$, where the equilibrium ion density $n_i^0(r) \equiv n(r)$ is defined by

$$n(r) = \int d^3v\ f_i^0(H_\perp + \omega_\theta P_\theta, H_{||}) . \tag{2}$$

The linearized continuity and momentum transfer equations for the cold fluid electrons can be expressed as

$$\frac{\partial}{\partial t}\,\delta n_e + \nabla \cdot (n\delta\underset{\sim}{V}_e) = 0 , \tag{3}$$

and

$$m_e \frac{\partial}{\partial t}\,\delta\underset{\sim}{V}_e = -e\left(\delta\underset{\sim}{E} + \frac{\delta\underset{\sim}{V}_e \times B_z^0\hat{\underset{\sim}{e}}_z}{c}\right), \tag{4}$$

where $\delta n_e(\underset{\sim}{x},t)$ is the perturbed electron density and $\delta\underset{\sim}{V}_e(\underset{\sim}{x},t)$ is the perturbed electron fluid velocity. Within the context of the assumptions enumerated in the previous paragraph, the perturbed electric

and magnetic fields, $\delta\underset{\sim}{E}(\underset{\sim}{x},t)$ and $\delta\underset{\sim}{B}(\underset{\sim}{x},t)$, are determined self-consistently from the Maxwell equations

$$\nabla \times \delta\underset{\sim}{E} = -\frac{1}{c}\frac{\partial}{\partial t}\delta\underset{\sim}{B} , \tag{5}$$

$$\nabla \times \delta\underset{\sim}{B} + \frac{4\pi}{c} e\int d^3v\, \underset{\sim}{v}\, \delta f_i(\underset{\sim}{x},\underset{\sim}{v},t) - \frac{4\pi e}{c} n\delta\underset{\sim}{V}_e(\underset{\sim}{x},t) , \tag{6}$$

and

$$\delta n_i(\underset{\sim}{x},t) = \delta n_e(\underset{\sim}{x},t) , \tag{7}$$

where $\nabla \cdot \delta\underset{\sim}{B} = 0$, and $\delta n_i(\underset{\sim}{x},t) = \int d^3v\, \delta f_i(\underset{\sim}{x},\underset{\sim}{v},t)$ is the perturbed ion density. Consistent with first-order charge neutrality [Eq. (7)], we choose a gauge in which the perturbed electric and magnetic fields are expressed as $\delta\underset{\sim}{E}(\underset{\sim}{x},t) = -c^{-1}(\partial/\partial t)\delta\underset{\sim}{A}(\underset{\sim}{x},t)$ and $\delta\underset{\sim}{B}(\underset{\sim}{x},t) = \nabla \times \delta\underset{\sim}{A}(\underset{\sim}{x},t)$, with $\nabla \cdot \delta\underset{\sim}{A} = 0$.

It is convenient to introduce the Lagrangian displacement vector $\underset{\sim}{\xi}(\underset{\sim}{x},t)$ defined by

$$\delta\underset{\sim}{V}_e(\underset{\sim}{x},t) = \frac{\partial}{\partial t}\underset{\sim}{\xi}(\underset{\sim}{x},t) . \tag{8}$$

Substituting Eq. (8) into Eq. (4) and integrating with respect to t, we find

$$\delta\underset{\sim}{A}(\underset{\sim}{x},t) = (m_e c/e)(\partial/\partial t)\underset{\sim}{\xi} + \underset{\sim}{\xi} \times \underset{\sim}{B}^0 , \tag{9}$$

where $\underset{\sim}{B}^0 = B_z^0(r)\hat{\underset{\sim}{e}}_z$. Moreover, integrating Eq. (3) with respect to t gives

$$\delta n_e(\underset{\sim}{x},t) = -\nabla \cdot [n(r)\underset{\sim}{\xi}(\underset{\sim}{x},t)] , \tag{10}$$

for the perturbed electron density.

In the subsequent analysis, it is assumed that all perturbed quantities vary according to $\delta\psi(\underset{\sim}{x},t) = \hat{\psi}(r)\exp(ik_z z - i\omega t)$, where ω is the complex oscillation frequency, and k_z is the (real) axial wavenumber of the perturbation. Moreover, we examine the class of purely growing modes with $\mathrm{Re}\omega = 0$, and consider the state corresponding to marginal stability with $\mathrm{Im}\omega = 0$. Imposing the condition

$$\omega = 0 \ , \tag{11}$$

and assuming azimuthally symmetric perturbations ($\partial/\partial\theta = 0$), then $\nabla \cdot \hat{\underset{\sim}{A}} = 0$ and $\hat{\underset{\sim}{A}} = \hat{\underset{\sim}{\xi}} \times \underset{\sim}{B}^0$ [Eq. (9)] can be combined to give

$$\begin{aligned} \hat{A}_r(r) &= \hat{A}_z(r) = 0 \ , \\ \hat{\xi}_\theta(r) &= 0 \ , \\ \hat{\xi}_r(r) &= -\hat{A}_\theta(r)/B_z^0(r) \ , \end{aligned} \tag{12}$$

at marginal stability. Moreover, making use of $\delta\underset{\sim}{B} = \nabla \times \delta\underset{\sim}{A}$ and Eq. (12), we find

$$\begin{aligned} \hat{B}_r(r) &= -ik_z\hat{A}_\theta(r) \ , \\ \hat{B}_\theta(r) &= 0 \ , \\ \hat{B}_z(r) &= \frac{1}{r}\frac{\partial}{\partial r}\left[r\hat{A}_\theta(r)\right] \ . \end{aligned} \tag{13}$$

In addition, the perturbed electric field is $\delta\underset{\sim}{E} = i(\omega/c)\delta\underset{\sim}{A} = 0$ for $\omega = 0$. In order to evaluate the perturbed ion distribution function δf_i [Eq. (1)], we note from Eq. (13) that $\underset{\sim}{v} \times \hat{\underset{\sim}{B}} \cdot (\partial/\partial\underset{\sim}{v}) f_i^0(H_\perp + \omega_\theta P_\theta, H_{||}) = m_i\omega_\theta r\hat{\underset{\sim}{e}}_\theta \cdot \underset{\sim}{v} \times \hat{\underset{\sim}{B}}\,(\partial f_i^0/\partial H_\perp) + m_i v_z\hat{\underset{\sim}{e}}_z \cdot \underset{\sim}{v} \times \hat{\underset{\sim}{B}}\,(\partial f_i^0/\partial H_{||} - \partial f_i^0/\partial H_\perp) = -m_i\omega_\theta(\partial f_i^0/\partial H_\perp)[ik_z v_z r\hat{A}_\theta + v_r(\partial/\partial r)(r\hat{A}_\theta)] + m_i v_\theta(\partial f_i^0/\partial H_{||} - \partial f_i^0/\partial H_\perp) \times ik_z v_z\hat{A}_\theta$. Defining $\delta f_i(\underset{\sim}{x},\underset{\sim}{v},t) = \hat{f}_i(r,\underset{\sim}{v})\exp(ik_z z - i\omega t)$, Eq. (1) then gives

$$\hat{f}_i(r,\underset{\sim}{v}) = \frac{e\omega_\theta}{c}\frac{\partial f_i^0}{\partial H_\perp}\int_{-\infty}^{t} dt' \exp[ik_z(z' - z)]$$

$$\times \{ik_z v_z' r' \hat{A}_\theta(r') + v_r' \frac{\partial}{\partial r'}[r'\hat{A}_\theta(r')]\} \qquad (14)$$

$$- \frac{e}{c}\left(\frac{\partial f_i^0}{\partial H_{||}} - \frac{\partial f_i^0}{\partial H_\perp}\right)\int_{-\infty}^{t} dt' \exp[ik_z(z' - z)]$$

$$\times ik_z v_z' v_\theta' \hat{A}_\theta(r') \ ,$$

for $\omega = 0$. The first integrand on the right-hand side of Eq. (14) can also be expressed as $(d/dt')\{r'\hat{A}_\theta(r')\exp[ik_z(z' - z)]\} = \underset{\sim}{v}' \cdot \underset{\sim}{\nabla}' \times \{r\hat{A}_\theta(r')\exp[ik_z(z' - z)]\}$for $\omega = 0$. Integrating with respect to t', Eq. (14) gives

$$\hat{f}_i(r,\underset{\sim}{v}) = \frac{e\omega_\theta}{c} r\hat{A}_\theta(r)\frac{\partial f_i^0}{\partial H_\perp}$$

$$- \frac{e}{c}\left(\frac{\partial f_i^0}{\partial H_{||}} - \frac{\partial f_i^0}{\partial H_\perp}\right)\int_{-\infty}^{t} dt' \exp[ik_z(z' - z)]ik_z v_z' v_\theta' \hat{A}_\theta(r') \ , \qquad (15)$$

where use has been made of $\underset{\sim}{x}'(t' = t) = \underset{\sim}{x}$. Making use of $ik_z v_z' \exp \times [ik_z(z' - z)]v_\theta'\hat{A}_\theta(r') = (d/dt' - v_r'\partial/\partial r') \times \exp[ik_z(z' - z)]v_\theta'\hat{A}_\theta(r')$ for $\partial/\partial t' = 0$ and $\partial/\partial\theta' = 0$, Eq. (15) can also be expressed as

$$\hat{f}_i(r,\underset{\sim}{v}) = \frac{e\omega_\theta}{c} r\hat{A}_\theta(r)\frac{\partial f_i^0}{\partial H_\perp}$$

$$- \frac{e}{c}\left(\frac{\partial f_i^0}{\partial H_{||}} - \frac{\partial f_i^0}{\partial H_\perp}\right)[v_\theta\hat{A}_\theta(r) + S_{r\theta}] \ , \qquad (16)$$

where the orbit integral $S_{r\theta}(k_z,\underset{\sim}{v},r)$ is defined by

$$S_{r\theta} = -\int_{-\infty}^{t} dt' \exp[ik_z(z' - z)]v_r' \frac{\partial}{\partial r'} v_\theta'\hat{A}_\theta(r') \ . \qquad (17)$$

Introducing the perturbed flux function $\hat{\psi}(r) = r\hat{A}_\theta(r)$ and making use of Eq. (16), the perturbed Maxwell equation (6) can be expressed as

$$r\frac{\partial}{\partial r}\left(\frac{1}{r}\frac{\partial}{\partial r}\hat{\psi}\right) - k_z^2\hat{\psi} + \frac{4\pi e^2\omega_\theta r}{c^2}\left(\int d^3v\, v_\theta \frac{\partial f_i^0}{\partial H_\perp}\right)\hat{\psi}$$
$$- \frac{4\pi e^2}{c^2}\int d^3v\, v_\theta\left(\frac{\partial f_i^0}{\partial H_{||}} - \frac{\partial f_i^0}{\partial H_\perp}\right)(v_\theta\hat{\psi} + rS_{r\theta}) = 0 , \tag{18}$$

with boundary conditions $\hat{\psi}(r = 0) = 0$ and $\lim_{r\to\infty}[r^{-1}(\partial/\partial r)\hat{\psi}(r)] = 0$. Moreover, from Eqs. (7), (10), and (16), the quasineutrality condition $\hat{n}_e(r) = \hat{n}_i(r)$ can be expressed as

$$ik_z n\hat{\xi}_z - \frac{1}{r}\frac{\partial}{\partial r}[n(\hat{\psi}/B_z^0)]$$
$$= -\frac{e\omega_\theta}{c}\hat{\psi}\left[\int d^3v(\partial f_i^0/\partial H_\perp)\right] \tag{19}$$
$$+ \frac{e}{c}\int d^3v\left(\frac{\partial f_i^0}{\partial H_{||}} - \frac{\partial f_i^0}{\partial H_\perp}\right)\left(v_\theta\frac{\hat{\psi}}{r} + S_{r\theta}\right) ,$$

where $n(r) = \int d^3v\, f_i^0$ is the equilibrium density profile and $B_z^0(r)$ is the equilibrium axial magnetic field.

The eigenvalue equations (18) and (19) are valid for purely growing modes at marginal stability ($Re\omega = 0 = Im\omega$) for the general class of rigid rotor ion equilibria $f_i^0(H_\perp + \omega_\theta P_\theta, H_{||})$. Moreover, as a procedural point, Eq. (18) can be used to determine the eigenfunction $\hat{\psi}(r)$. Equation (19) can then be used to determine the corresponding axial displacement $\hat{\xi}_z(r)$ self-consistently.

B. Eigenvalue Equation for Isotropic Ions

Equation (18) simplifies considerably in circumstances where the ion equilibrium $f_i^0(H_\perp + \omega_\theta P_\theta, H_{||})$ is isotropic with

$$f_i^0 = f_i^0(H_\perp + H_{||} + \omega_\theta P_\theta) \ . \tag{20}$$

In this case, $\partial f_i^0/\partial H_{||} = \partial f_i^0/\partial H_\perp$, and Eq. (18) reduces exactly to

$$r \frac{\partial}{\partial r} \left(\frac{1}{r} \frac{\partial}{\partial r} \hat{\psi}\right) - k_z^2 \hat{\psi} + \frac{4\pi e^2 \omega_\theta r}{c^2} \left(\int d^3v \ v_\theta \frac{\partial f_i^0}{\partial H_\perp} \right) \hat{\psi} = 0 \ . \tag{21}$$

Before examining Eq. (21) for a specific choice of ion distribution function f_i^0, it is useful to derive some equilibrium identities valid for general $f_i^0 (H_\perp + H_{||} + \omega_\theta P_\theta)$. First, noting that $H_\perp + H_{||} + \omega_\theta P_\theta = (m_i/2) \times [v_r^2 + (v_\theta + \omega_\theta r)^2 + v_z^2] - (m_i/2)\omega_\theta^2 r^2 + (e/c)(\omega_\theta r)A_\theta^0$, it follows that

$$\int d^3v \ v_\theta \frac{\partial f_i^0}{\partial H_\perp} = -\omega_\theta r \int d^3v \frac{\partial f_i^0}{\partial H_\perp} \ . \tag{22}$$

Second, making use of $n(r) = \int d^3v \ f_i^0(H_\perp + H_{||} + \omega_\theta P_\theta)$ and $B_z^0(r) = r^{-1}(\partial/\partial r)(rA_\theta^0)$, it is straightforward to show that

$$\frac{\partial}{\partial r} n(r) = -m_i \omega_\theta r \left(\omega_\theta - \frac{eB_z^0(r)}{m_i c} \right) \int d^3v \frac{\partial f_i^0}{\partial H_\perp} \ . \tag{23}$$

Substituting Eqs. (22) and (23) into Eq. (22), the marginal stability eigenvalue equation for the perturbed flux function $\hat{\psi}(r) = r\hat{A}_\theta(r)$ can be expressed in the equivalent form

$$r \frac{\partial}{\partial r} \left(\frac{1}{r} \frac{\partial}{\partial r} \hat{\psi}\right) - k_z^2 \hat{\psi} + \frac{4\pi e^2}{m_i c^2} \frac{\omega_\theta r \partial n(r)/\partial r}{\omega_\theta - eB_z^0(r)/m_i c} \hat{\psi} = 0 \ , \tag{24}$$

which is valid for the general class of isotropic rigid-rotor ion equilibria $f_i^0(H_\perp + H_{||} + \omega_\theta P_\theta)$.

C. Approximate Eigenvalue Equation for Anisotropic Ions

Because of the complexity of the orbit integral $S_{r\theta}$ in Eq. (18), the general eigenvalue equation for anisotropic ions is difficult to solve except in special limiting cases. We consider one such case

here that is of considerable practical interest. In particular, it is straightforward to show that the $S_{r\theta}$ contribution in Eqs. (16) and (18) can be neglected in comparison with $v_\theta \hat{A}_\theta(r)$ whenever $|k_z v_z \hat{A}_\theta| >> |v_r \partial \hat{A}_\theta/\partial r|$. Estimating $v_z \approx v_r \approx v_i$, where v_i is the characteristic ion thermal speed, and estimating $|\partial \ell n \hat{A}_\theta/\partial r|^{-1} \approx d$, where d is the characteristic radial scale length of the eigenfunction, we conclude that $S_{r\theta}$ can be neglected in comparison with $r\hat{A}_\theta$ when the inequality

$$|k_z d| >> 1 \tag{25}$$

is satisfied. In circumstances where Eq. (25) is satisfied and the orbit integral $S_{r\theta}$ can be neglected in Eq. (16), the eigenvalue equation (18) can be approximated by

$$r\frac{\partial}{\partial r}\left(\frac{1}{r}\frac{\partial}{\partial r}\hat{\psi}\right) - k_z^2\hat{\psi} + \frac{4\pi e^2 \omega_\theta r}{c^2}\left(\int d^3v\, v_\theta \frac{\partial f_i^0}{\partial H_\perp}\right)\hat{\psi} - \frac{4\pi e^2}{c^2}\left(\int d^3v\, v_\theta^2\left(\frac{\partial f_i^0}{\partial H_{||}} - \frac{\partial f_i^0}{\partial H_\perp}\right)\right)\hat{\psi} = 0 , \tag{26}$$

for general anisotropic ion equilibrium $f_i^0(H_\perp + \omega_\theta P_\theta, H_{||})$. Equation (26) of course reduces to Eq. (21) for the case of isotropic ions with $f_i^0 = f_i^0(H_\perp + H_{||} + \omega_\theta P_\theta)$.

As found numerically in Sec. III [Eq. (39) and Fig. 2], for a thin ion layer with mean radius r_0 much larger than the layer thickness δ, the characteristic k_z can be estimated by $k_z \approx k_0 \simeq r_0/\delta^2$ and the eigenfunction scale length by $d \approx \delta$. Therefore,

$$|k_z d| \approx k_0 \delta \simeq r_0/\delta >> 1 , \tag{27}$$

and the inequality is readily satisfied for a thin layer with $r_0 >> \delta$. We note from Eqs. (15) - (18) that Eq. (26) is equivalent to a model

eigenvalue equation in which the radial orbits are in effect assumed to be circular with $r' \simeq r$ and $v'_r = dr'/dt' \simeq 0$.

III. STABILITY PROPERTIES FOR GIBBS ION EQUILIBRIUM

A. Equilibrium Properties

To examine detailed stability properties, we specialize to the case where f_i^0 corresponds to the two-temperature Gibbs equilibrium

$$f_i^0 = \frac{n_0}{(2\pi T_\perp/m_i)} \frac{1}{(2\pi T_{||}/m_i)^{1/2}} \exp\left[-\frac{1}{T_\perp}(H_\perp + \omega_\theta P_\theta) - \frac{H_{||}}{T_{||}}\right], \qquad (28)$$

where n_0 = const., and $T_\perp$ = const. and $T_{||}$ = const. are the (uniform) perpendicular and parallel ion temperatures. From $n(r) = \int d^3v f_i^0$ and $\partial B_z^0/\partial r = (4\pi e/c)\omega_\theta r n(r)$, the equilibrium density and magnetic field profiles are given by the well-known expressions[6-8]

$$n(r) = n_0 \mathrm{sech}^2\left(\frac{r^2 - r_0^2}{2\delta^2}\right), \qquad (29)$$

and

$$B_z^0(r) = \frac{cT_\perp}{e\omega_\theta}\left[\frac{m_i\omega_\theta^2}{T} + \frac{2}{\delta^2}\tanh\left(\frac{r^2 - r_0^2}{2\delta^2}\right)\right], \qquad (30)$$

where $\delta^4 = 2c^2T_\perp/(m_i\omega_\theta^2\omega_{pi}^2)$, $\omega_{pi}^2 = 4\pi n_0 e^2/m_i$, and r_0^2 = const. Note from Eq. (29) that n_0 corresponds to the maximum ion density, which occurs at $r = r_0$. We denote the externally applied magnetic field by $B_0 = B_z^0(r \to \infty)$ and assume $B_0 > 0$ without loss of generality. It follows from Eq. (30) that the equilibrium exists only for $\omega_\theta > 0$. Moreover, B_0 is related to other equilibrium parameters by

$$\frac{eB_0}{m_i c}\omega_\theta = \omega_\theta^2 + v_i^2/\delta^2, \qquad (31)$$

where $v_i = (2T_\perp/m_i)^{1/2}$ is the ion thermal speed, and $v_i^2/\delta^2 = (v_i/c)\omega_\theta\omega_{pi}$. Evaluating Eq. (30) at $r = 0$ gives

$$\frac{eB_z^0(0)}{m_i c}\omega_\theta = \omega_\theta^2 - \frac{v_i^2}{\delta^2}\tanh\frac{r_0^2}{2\delta^2}. \qquad (32)$$

Subtracting Eq. (32) from Eq. (31), the fractional magnetic field depression can be expressed as[8]

$$\frac{B_0 - B_z(0)}{B_0} = \beta_i^{1/2}[1 + \tanh(r_0^2/2\delta^2)] \ , \tag{33}$$

where $\beta_i = 8\pi n_0 T_\perp / B_0^2$ is the ratio of perpendicular ion pressure ($n_0 T_\perp$) at $r = r_0$ to magnetic pressure ($B_0^2/8\pi$) as $r \to \infty$. Equation (33) is a useful identity relating the normalized layer radius (r_0/δ) to β_i and $[B_0 - B_z(0)]/B_0$.

B. Stability Behavior for Isotropic Ions

In this section, we make use of the eigenvalue equation (21) to investigate stability properties for the case of an isotropic ion equilibrium with $T_\perp = T_{||}$ and $\partial f_i^0/\partial H_\perp = \partial f_i^0/\partial H_{||}$ in Eq. (28). To analyze the marginal eigenvalue equation (21), it is convenient to introduce the dimensionless quantities

$$R = r/\delta \ , \quad R_0 = r_0/\delta \ , \quad k^2 = k_z^2\delta^2 \ . \tag{34}$$

Substituting Eqs. (22), (28), and (29) into Eq. (21), the eigenvalue equation for $\hat{\psi} = r\hat{A}_\theta$ can be expressed in the form of a Schroedinger equation for $\hat{A}_\theta$, i.e.,

$$\frac{1}{R}\frac{\partial}{\partial R} R \frac{\partial}{\partial R} \hat{A}_\theta + \left[-k^2 - \frac{1}{R^2} + 2R^2 \operatorname{sech}^2\left(\frac{R^2 - R_0^2}{2}\right)\right]\hat{A}_\theta = 0 \ , \tag{35}$$

with boundary conditions $[r\hat{A}_\theta]_{R=0} = 0$ and $\lim_{R\to\infty}[R^{-1}(\partial/\partial R)(R\hat{A}_\theta)] = 0$. From Eq. (35), $-k^2 = E$ plays the role of the energy eigenvalue, and the effective potential in cylindrical coordinates is

$$V(R) = \frac{1}{R^2} - 2R^2 \operatorname{sech}^2\left(\frac{R^2 - R_0^2}{2}\right) \ . \tag{36}$$

Near the origin ($R^2 << k^2$), the solution to Eq. (35) can be approximated by

$$R\hat{A}_\theta = ARI_1[(k^2R^2)^{1/2}] , \tag{37}$$

where A is a constant coefficient, and $I_1(x)$ is the modified Bessel function of the first kind of order unity. On the other hand, for $R >> R_0$, the asymptotic solution to Eq. (35) is given by

$$R\hat{A}_\theta \simeq B\sqrt{\pi/2}(R^2/k^2)^{1/4}\exp[-(k^2R^2)^{1/2}] , \tag{38}$$

where B is a constant.

The effective potential V(R) [Eq. (36)] is illustrated in Fig. 1 for $R_0 = r_0/\delta = 3$. Note that the eigenvalue equation (35) not only determines the eigenfunction $\hat{A}_\theta(R)$ at marginal stability but also determines the discrete (quantized) value of normalized axial wavenumber-squared (denote by $k^2 \equiv k_0^2\delta^2$) corresponding to $Im\omega = 0$.

The eigenvalue equation (35) has been solved numerically for R_0^2 in the range $0 \leq R_0^2 < 10$. For each value of R_0^2, it is found that there is only one allowed value of $k_0^2\delta^2$, corresponding to a single bound energy eigenstate. The numerical results are summarized in Fig. 2, where the eigenvalue $k_0^2\delta^2$ is plotted as a function of R_0^2. The same information is presented in Fig. 3, where Eq. (33) and the information in Fig. 2 are used to plot $k_0^2\delta^2$ versus the normalized magnetic field depression $\beta_i^{-1/2}[B_0 - B_z^0(0)]/B_0$. The universal curves in Figs. 2 and 3 determine the critical wavenumber $k_0^2\delta^2$ corresponding to marginal stability ($Im\omega = 0$). In particular, purely growing (and purely damped) solutions exist for axial wavenumber k_z in the range $0 < k_z^2 < k_0^2$.[9] On the other hand, $Im\omega = 0$ for $k_z^2 \geq k_0^2$, and $Re\omega$ is generally non-zero.[9]

Figures 4 and 5 illustrate the equilibrium profiles n(r) [Eq. (29)] and $B_z^0(r)$ [Eq. (30)] and the eigenfunction $r\hat{A}_\theta(r)$ at marginal stability [Eq. (35)] for the two cases $r_0/\delta = 1$ [Fig. 4] and $r_0/\delta = 3$ [Fig. 5], and for $\beta_i = 1$ (maximum field depression). We note from Figs. 4 and 5 that the eigenfunction $r\hat{A}_\theta(r)$ is strongly peaked about $r \approx r_0$ for $r_0/\delta >> 1$, and that V(R) is strongly peaked for $r_0/\delta >> 1$ [Fig. 1]. We also note from Figure 2, that $k_0^2\delta^2$ can be approximated by

$$k_0^2\delta^2 = r_0^2/\delta^2 \ , \tag{39}$$

to a high degree of accuracy, for $r_0^2/\delta^2 > 1$.

C. Stability Behavior for Anisotropic Ions

In this section, we make use of the approximate eigenvalue equation (26) to investigate stability properties for the case of an anisotropic ion equilibrium with $T_{\parallel} > T_{\perp}$ in Eq. (28). As discussed in Sec. II.C, the approximate eigenvalue equation (26) is expected to be a good approximation to the exact eigenvalue equation (18) in circumstances where the ion layer is thin ($r_0 >> \delta$) and the orbits are nearly circular. Introducing the dimensionless quantities defined in Eq. (34), and substituting Eqs. (22), (28), and (29) into Eq. (26), the eigenvalue equation for $\hat{A}_\theta$ can be expressed as

$$\frac{1}{R}\frac{\partial}{\partial R} R \frac{\partial}{\partial R} \hat{A}_\theta + \left[-k^2 - \frac{1}{R^2} + 2R^2 \operatorname{sech}^2\left(\frac{R^2 - R_0^2}{2}\right) - \left(1 - \frac{T_\perp}{T_\parallel}\right)\left(\frac{\omega_{pi}^2 \delta^2}{c^2} + 2R^2\right) \operatorname{sech}^2\left(\frac{R^2 - R_0^2}{2}\right)\right] \hat{A}_\theta = 0 , \tag{40}$$

with boundary conditions $[R\hat{A}_\theta]_{R=0} = 0$ and $\lim_{R\to\infty} [R^{-1}(\partial/\partial R)(R\hat{A}_\theta)] = 0$. In Eq. (40), the dimensionless quantity $\omega_{pi}^2\delta^2/c^2$ can also be expressed as

$$\frac{\omega_{pi}^2 \delta^2}{c^2} = \frac{\omega_{ci} - \omega_\theta}{\omega_\theta} , \tag{41}$$

where $\omega_{ci} = eB_0/m_i c$, and use has been made of $\delta^4 = 2c^2 T_\perp/(m_i \omega_\theta^2 \omega_{pi}^2)$ and Eq. (31).

Analogous to Eq. (35) for an isotropic ion equilibrium, the eigenvalue equation (40) has the form of a Schroedinger equation with $-k^2$ playing the role of the energy eigenvalue and effective potential $V(R)$ defined by

$$V(R) = \frac{1}{R^2} - 2R^2 \operatorname{sech}^2\left(\frac{R^2 - R_0^2}{2}\right) + \left(1 - \frac{T_\perp}{T_\parallel}\right)\left(\frac{\omega_{ci} - \omega_\theta}{\omega_\theta} + 2R^2\right) \times \operatorname{sech}^2\left(\frac{R^2 - R_0^2}{2}\right) . \tag{42}$$

The effective potential V(R) is illustrated in Fig. 6 for $r_0/\delta = 3$, $\omega_\theta/\omega_{ci} = 0.01$, and $T_\perp/T_{||} = 0.9$. As a general remark, Eq. (42) shows that temperature anisotropy with $T_{||} > T_\perp$ has the effect of reducing the depth of the effective potential. For fixed r_0/δ, this in turn reduces the critical value of $k_z^2\delta^2$ for marginal stability.

Near the origin ($R^2 \ll k_z^2\delta^2$), the solution to Eq. (40) is

$$R\hat{A}_\theta \simeq C_1 R I_1[(\hat{k}^2R^2)^{1/2}] , \tag{43}$$

where C_1 is a constant, I_1 is the modified Bessel function of the first kind of order unity, and $\hat{k}^2$ is defined by

$$\hat{k}^2 \equiv k_z^2\delta^2 + 2\left(\frac{\omega_{pi}^2\delta^2}{c^2}\right)\left(1 - \frac{T_\perp}{T_{||}}\right) \operatorname{sech}^2\left(\frac{R_0^2}{2}\right) .$$

For $R \gg R_0$, the solution to Eq. (40) is

$$R\hat{A}_\theta \simeq C_2(R^2/k^2)^{1/4}\exp[-(k^2R^2)^{1/2}] , \tag{44}$$

where C_2 is a constant.

The full solution to the marginal stability eigenvalue equation (40) requires numerical analysis. Equation (40) has been solved numerically for $(r_0/\delta)^2$ in the range $0 < r_0^2/\delta^2 < 16$. As in the case of an isotropic ion equilibrium, for each value of r_0/δ it is found that there is one eigenvalue $k_0^2\delta^2$ for which a solution exists to Eq. (40) satisfying the appropriate boundary conditions. Consistent with the fact that the effective potential well depth decreases for $T_{||}/T_\perp > 1$, for a fixed value of r_0/δ it is found that the temperature anisotropy reduces the value of critical wavenumber $k_0\delta$ for marginal stability. Numerical results are summarized in Figs. 7 and 8 where the eigenvalue $k_0^2\delta^2$ is plotted versus r_0^2/δ^2 for $\omega_{ci}/\omega_\theta = 50$, 100, and several values of $T_\perp/T_{||}$. Figures 7 and 8 show that the stabilizing influence

of temperature anisotropy increases as $T_{||}/T_{\perp}$ increases. Physically, the perturbation described by Eq. (15) corresponds to a density and current modulation. By examining δJ_{θ}^{i}, δA_{r}, and δA_{θ} in detail, we find that the perturbation produces a $J_{\theta 0}^{i} \times \delta B_{r}$ force which increases the amplitudes of the current modulation. Of course, this force is in the axial direction. For $T_{||} >> T_{\perp}$, however, the greater axial pressure $P_{||}$ tends to inhibit the growth of the perturbation.

The numerical analysis also shows that the stabilizing influence of $T_{||} > T_{\perp}$ tends to decrease as $\omega_{\theta}/\omega_{ci}$ decreases. This effect is illustrated in Fig. 9 where $(T_{\perp}/T_{||})_{cr}$ is plotted versus r_0^2/δ^2 for several values of $\omega_{ci}/\omega_{\theta}$. Here, $(T_{\perp}/T_{||})_{cr}$ is the critical value of $(T_{\perp}/T_{||})$ for which the eigenvalue $k_0^2\delta^2 = 0$, thereby reducing the range of unstable k_z-values to zero. The following point is also noteworthy. For fixed r_0/δ, the degree of field-reversal increases as $\omega_{\theta}/\omega_{ci}$ decreases [Eqs. (31) and (33)]. Therefore, a higher degree of field-reversal requires less temperature anisotropy for stabilization. This is confirmed by the numerical results. Shown in Fig. 10 is a plot of $(T_{\perp}/T_{||})_{cr}$ versus $B_z(0)/B_0$ in the range $-1 \leq B_z(0)/B_0 \leq 0$, for various values of r_0^2/δ^2. Figure 10 relates the critical value of $T_{\perp}/T_{||}$ required for stabilization to the magnetic field depression on axis.

Finally, it is important to note from Figs. 7 and 8 that large eigenvalues $k_0^2\delta^2$ correspond to large values of r_0/δ. Therefore, the results in this section are consistent with the thin-layer approximation. On the other hand, an examination of the exact eigenvalue equation (15) shows that the orbit integral contribution vanishes identically in the limit of small $k_z\delta$. Thus, the approximations used

to obtain the eigenvalue equation (26) break down in the limit $k_z \to 0$. Therefore, the values of $(T_\perp/T_{||})_{cr}$ calculated in this section should only be viewed in an approximate sense.

IV. CONCLUSIONS

In this paper we have investigated tearing-mode stability properties at marginal stability for the specific choice of ion distribution function $f_i^0(H_\perp + \omega_\theta P_\theta, H_{||})$ corresponding to the anisotropic equilibrium in Eq. (28). In the isotropic case with $T_\perp = T_{||}$ [Secs. II.B and III.B], the general eigenvalue equation (18) reduced exactly to Eq. (35) for the choice of equilibrium distribution function in Eq. (28). In Sec. III.B, Eq. (35) was solved numerically for both the eigenfunction $\hat{A}_\theta(R)$ and the eigenvalue (denoted by $k_0^2\delta^2$) as a function of various equilibrium parameters. This procedure determined the critical axial wavenumber k_0 corresponding to marginal stability ($Im\omega = 0$). For $T_\perp = T_{||}$ and $r_0^2/\delta^2 > 1$, the analysis showed that $k_0^2\delta^2$ can be approximated by $k_0^2\delta^2 = r_0^2/\delta^2$ [Eq. (39)] to a high degree of accuracy. In the anisotropic case with $T_\perp$ generally not equal to $T_{||}$ [Secs. II.C and III.C], the general eigenvalue equation (18) can be approximated by Eq. (40) in circumstances where the ion layer is thin ($r_0/\delta >> 1$) and the equilibrium distribution function is specified by Eq. (28). From the expression for the effective potential V(R) in Eq. (42), it is evident that temperature anisotropy with $T_{||} > T_\perp$ has the effect of <u>reducing</u> the depth of the potential well, and thereby reducing the value of $k_0^2\delta^2$ corresponding to marginal stability. Equation (40) was solved numerically in Sec. III.C for a broad range of system parameters. Marginal stability properties were investigated in detail as a function of $\omega_\theta/\omega_{ci}$, $T_{||}/T_\perp$ and r_0^2/δ^2, and estimates were made of the critical value of $T_{||}/T_\perp$ required for complete stabilization (reduction of k_0^2 to zero).

Finally, it is important to note that the present analysis can readily be extended to treat the electrons (as well as the ions) in a fully kinetic manner. This has the important effect of removing singular behavior in $\hat{\xi}_z(r)$ [Eq. (19)] and $\hat{\xi}_r(r)$ [Eq. (12)] as $B_z(r)$ passes through zero, as well as incorporating the full physics influence of kinetic electrons. To illustrate this simple extension, we consider the case of an isotropic electron equilibrium specified by

$$f_e^0 = \frac{n_0}{(2\pi T_e/m_e)^{3/2}} \exp[-(H_\perp + H_{||} + \omega_{\theta e} P_\theta)/T_e] , \qquad (45)$$

where T_e and $\omega_{\theta e}$ are constants, $H_\perp + H_{||} = (m_e/2)[v_r^2 + v_\theta^2 + v_z^2 - e\phi_0(r)]$ is the electron energy, $P_\theta = m_e r v_\theta - (e/c) r A_\theta^0(r)$ is the canonical angular momentum, and $-e$ and m_e are the electron charge and rest mass, respectively. From Eq. (45), for finite m_e and T_e, we note that it is generally necessary to allow for nonzero radial electric field $E_r^0 = -\partial\phi_0/\partial r$. For present purposes, we also assume that the ions are isotropic with f_i^0 specified by

$$f_i^0 = \frac{n_0}{(2\pi T_i/m_i)^{3/2}} \exp[-(H_\perp + H_{||} + \omega_{\theta i} P_\theta)/T_i] , \qquad (46)$$

where $H_\perp + H_{||} = (m_i/2)(v_r^2 + v_\theta^2 + v_z^2) + e\phi_0(r)$ is the ion energy, and $P_\theta = m_i r v_\theta - (e/c) r A_\theta^0(r)$ is the canonical angular momentum. For the choices of f_i^0 and f_e^0 in Eqs. (45) and (46) it is straightforward to show that the generalization of Eq. (21) to include kinetic electrons is given by

$$r \frac{\partial}{\partial r}\left(\frac{1}{r}\frac{\partial}{\partial r}\hat{\psi}\right) - k_z^2\hat{\psi} - \frac{4\pi e^2}{c^2}\left(\frac{\omega_{\theta i}^2}{T_i} + \frac{\omega_{\theta e}^2}{T_e}\right) r^2 n(r)\hat{\psi} = 0, \qquad (47)$$

where $n(r) \equiv n_i(r) = n_e(r)$. Making use of the definitions $n_i(r) = \int d^3v\, f_i^0$ and $n_e(r) = \int d^3v\, f_e^0$, and imposing equilibrium charge neutrality $n_i(r) = n_e(r)$ at each radial point, we find that $A_\theta^0(r)$ and $\phi_0(r)$ are related by

$$\frac{1}{T_i}\left(\frac{m_i}{2}\omega_{\theta i}^2 r^2 - \frac{e}{c}\omega_{\theta i} r A_\theta^0(r) - e\phi_0(r)\right)$$

$$= \frac{1}{T_e}\left(\frac{m_e}{2}\omega_{\theta e}^2 r^2 + \frac{e}{c}\omega_{\theta e} r A_\theta^0(r) + e\phi_0(r)\right), \tag{48}$$

or equivalently,

$$e\phi_0(r) = \left(\frac{1}{T_e} + \frac{1}{T_i}\right)^{-1}\left[\left(\frac{m_i\omega_{\theta i}^2}{2T_i} - \frac{m_e\omega_{\theta e}^2}{2T_e}\right)r^2 - \frac{e}{c}\left(\frac{\omega_{\theta i}}{T_i} - \frac{\omega_{\theta e}}{T_e}\right) r A_\theta^0\right]. \tag{49}$$

Note that Eq. (48) in effect determines the equilibrium electrostatic potential $\phi_0(r)$ in terms of $A_\theta^0(r)$, $\omega_{\theta i}$, $\omega_{\theta e}$, etc. The equilibrium axial magnetic field $B_z^0(r)$ is calculated from $\partial B_z^0(r)/\partial r = (4\pi e/c) \times (\omega_{\theta i} - \omega_{\theta e}) r n(r)$, where $n(r) = \int d^3v\, f_i^0$ can be expressed as

$$n(r) = n_0 \exp[(m_i\omega_{\theta i}^2 r^2/2 - e\omega_{\theta i} r A_\theta^0/c - e\phi_0)/T_i]$$

$$= n_0 \exp\left[\frac{(m_i\omega_{\theta i}^2 + m_e\omega_{\theta e}^2)}{T_e + T_i}\frac{r^2}{2} - \frac{e}{c}\frac{(\omega_{\theta i} - \omega_{\theta e})}{T_e + T_i} r A_\theta^0(r)\right]. \tag{50}$$

In obtaining Eq. (50) use has been made of Eq. (49) to eliminate $\phi_0(r)$. Solving $\partial B_z^0/\partial r = (4\pi e/c)(\omega_{\theta i} - \omega_{\theta e}) r n(r)$, we find that

$$n(r) = n_0 \operatorname{sech}^2\left(\frac{r^2 - r_0^2}{2\delta^2}\right), \tag{51}$$

and

$$B_z^0(r) = \frac{c(T_e + T_i)}{e(\omega_{\theta i} - \omega_{\theta e})}\left[\frac{m_i\omega_{\theta i}^2 + m_e\omega_{\theta e}^2}{T_e + T_i} + \frac{2}{\delta^2}\tanh\left(\frac{r^2 - r_0^2}{2\delta^2}\right)\right], \tag{52}$$

are the appropriate generalizations of Eqs. (29) and (30). Here $r_0^2 = \text{const.}$, and δ is defined by $\delta^4 = (2c^2/4\pi n_0 e^2)(T_e + T_i)/(\omega_{\theta i} - \omega_{\theta e})^2$. It is clear from Eqs. (46), (51), and (52) that the resulting eigenvalue equation and marginal stability analysis including electron kinetic effects exactly parallel the work in Sec. III.B with appropriate redefinition of constant coefficients and scaling parameters.

ACKNOWLEDGMENTS

This research was supported in part by the Office of Naval Research.

REFERENCES

1. C. A. Kapetanakos, J. Golden, J. A. Pasour, S. J. Marsh, and R. A. Mahaffey, Phys. Rev. Lett., to be published (1980).
2. S. J. Marsh, A. T. Drobot, J. Golden, and C. A. Kapetanakos, Phys. Fluids 21, 1045 (1978).
3. R. N. Sudan and E. Ott, Phys. Rev. Lett. 33, 355 (1974).
4. H. H. Fleischmann and T. Kammash, Nucl. Fusion 15, 1143 (1975).
5. C. A. Kapetanakos, J. Golden, and K. R. Chu, Plasma Phys. 19, 387 (1977).
6. K. D. Marx, Phys. Fluids 11, 357 (1968).
7. J. P. Freidberg and R. L. Morse, Phys. Fluids 12, 887 (1969).
8. J. Chen and R. C. Davidson, Phys. Fluids 23, 302 (1980).
9. H. S. Uhm and R. C. Davidson, Phys. Fluids 23, 348 (1980).
10. R. N. Sudan, Phys. Rev. Lett. 41, 476 (1978).
11. S. A. Goldstein, D. P. Bacon, D. Mosher, and G. Cooperstein, in Proceedings of the 2nd International Topical Conference on High Power Electron and Ion Beam Research and Technology (Cornell University, Ithaca, New York, 1977), Vol. I, p. 71; R. L. Martin, ibid., Vol. 1, p. 113.
12. M. J. Clauser, Phys. Rev. Lett. 35, 848 (1975).
13. J. W. Shearer, Nucl. Fusion 15, 952 (1975).
14. S. Humphries, R. N. Sudan, and L. Wiley, J. Appl. Phys. 47, 2382 (1976).
15. A. W. Maschke, IEEE Trans. Nucl. Sci. 22, 1825 (1975).
16. R. Burke, Y. Cho, J. Fasolo, S. Fenster, M. Fors, T. Khoe, A. Langsdorf, and R. Martin, IEEE Trans. Nucl. Sci. NS-24, 1012 (1977).
17. F. Winterberg, Phys. Rev. Lett. 37, 713 (1976).
18. J. P. Freidberg, Phys. Fluids 15, 1102 (1972).
19. R. C. Davidson, H. S. Uhm, and R. Aamodt, Phys. Fluids 22, 2158 (1979).

FIGURE CAPTIONS

Fig. 1 Plot of effective potential V(R) versus R = r/δ for $r_0/\delta = 1$ and $r_0/\delta = 3$ [Eq. (36)].

Fig. 2 Normalized critical wavenumber $k_0^2\delta^2$ [Eq. (35)] plotted versus r_0^2/δ^2.

Fig. 3 Normalized critical wavenumber $k_0^2\delta^2$ [Eq. (35)] plotted versus $\beta_i^{-1/2}[B_0 - B_z^0(0)]/B_0$.

Fig. 4 Plot of (a) $n(r)/n_0$ [Eq. (29)], (b) $B_z^0(r)/B_0$ [Eq. (30)], and (c) $r\hat{A}_\theta(r)$ [Eq. (35)] versus r/δ for $r_0/\delta = 1.0$, $\beta_i = 1.0$, and $k_0^2\delta^2 = 0.68$.

Fig. 5 Plot of (a) $n(r)/n_0$ [Eq. (29)], (b) $B_z^0(r)/B_0$ [Eq. (30)], and (c) $r\hat{A}_\theta(r)$ [Eq. (35)] versus r/δ for $r_0/\delta = 3.0$, $\beta_i = 1.0$, and $k_0^2\delta^2 = 8.95$.

Fig. 6 Plot of V(R) [Eq. (42)] versus R for $r_0/\delta = 3$, $\omega_{ci}/\omega_\theta = 100$, and (a) $T_\perp/T_{||} = 0.9$, and (b) $T_\perp/T_{||} = 1$.

Fig. 7 Plot of $k_0^2\delta^2$ versus r_0^2/δ^2 for $\omega_{ci}/\omega_\theta = 50$ and several values of $T_\perp/T_{||}$ [Eq. (40)].

Fig. 8 Plot of $k_0^2\delta^2$ versus r_0^2/δ^2 for $\omega_{ci}/\omega_\theta = 100$ and several values of $T_\perp/T_{||}$ [Eq. (40)].

Fig. 9 Plot of $(T_\perp/T_{||})_{cr}$ versus r_0^2/δ^2 for $\omega_{ci}/\omega_\theta = 100, 50, 10, 1$.

Fig. 10 Plot of $(T_\perp/T_{||})_{cr}$ versus $B_z(0)/B_0$ for $r_0^2/\delta^2 = 4, 10, 20$.

Fig. 11 Plot of eigenfunction $r\hat{A}_\theta$ versus r/δ [Eq. (40)] for $\omega_{ci}/\omega_\theta = 100$ and (a) $T_\perp/T_{||} = 1$ and (b) $T_\perp/T_{||} = 0.9$.

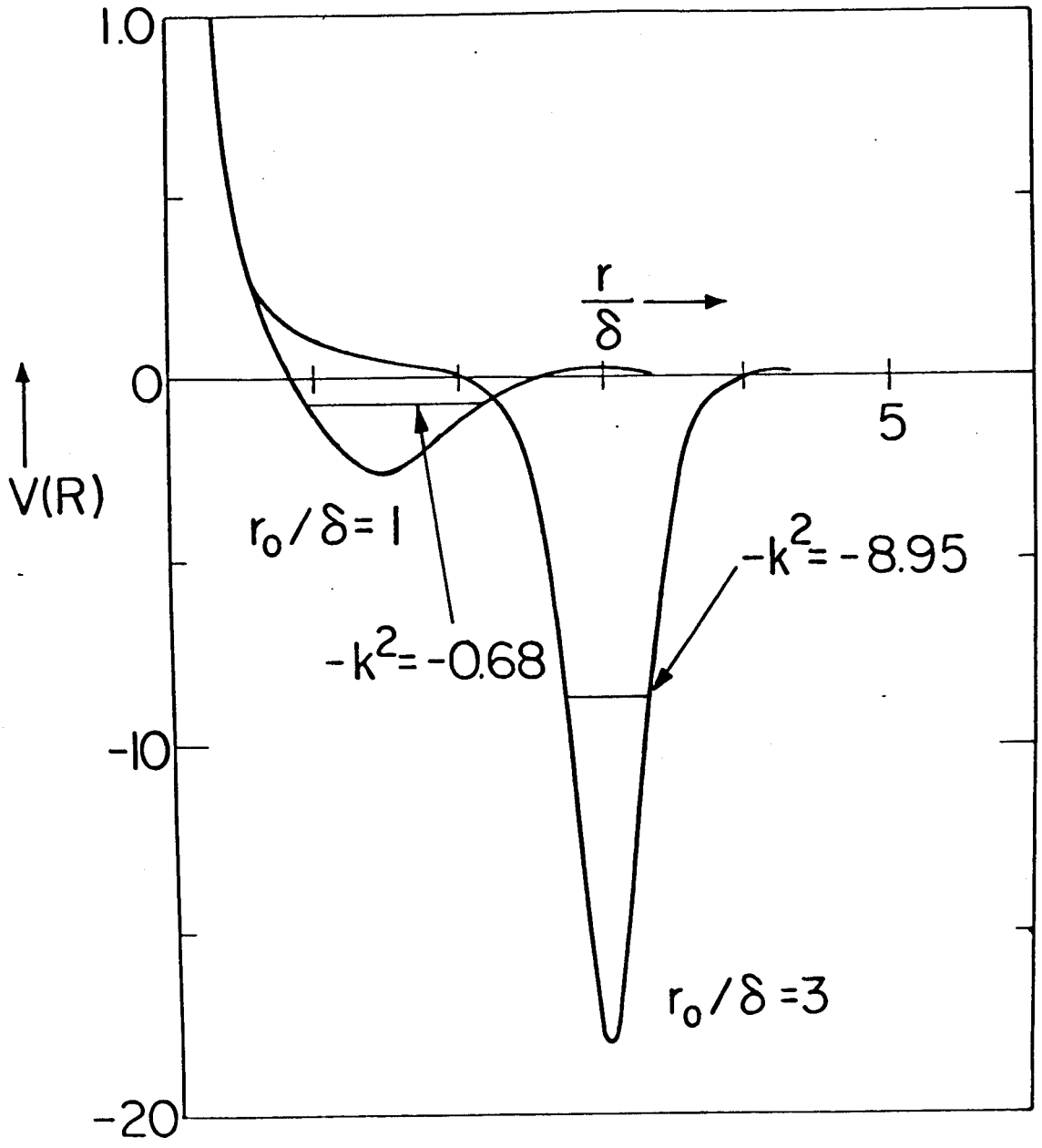

Figure 1.

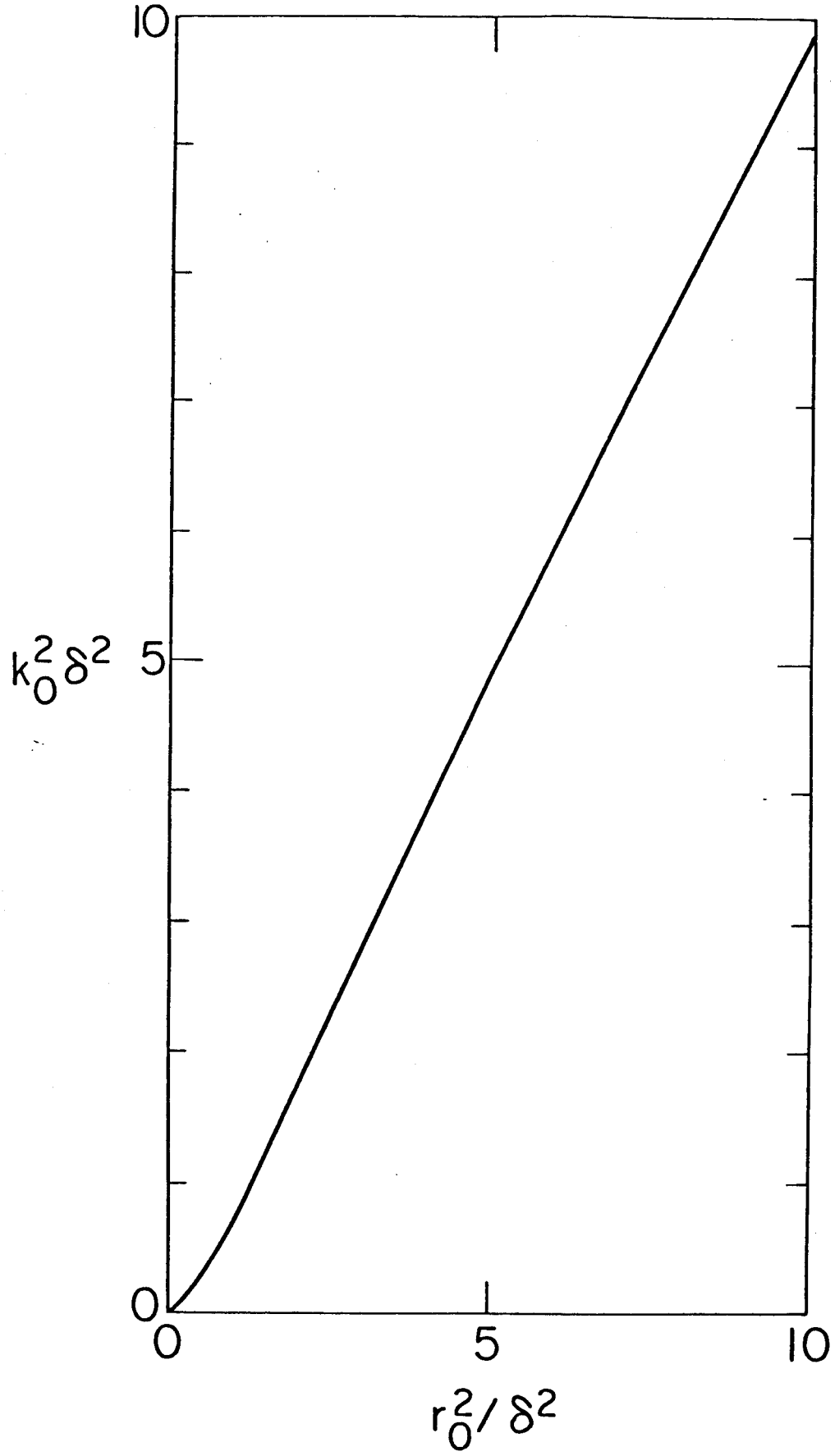

Figure 2.

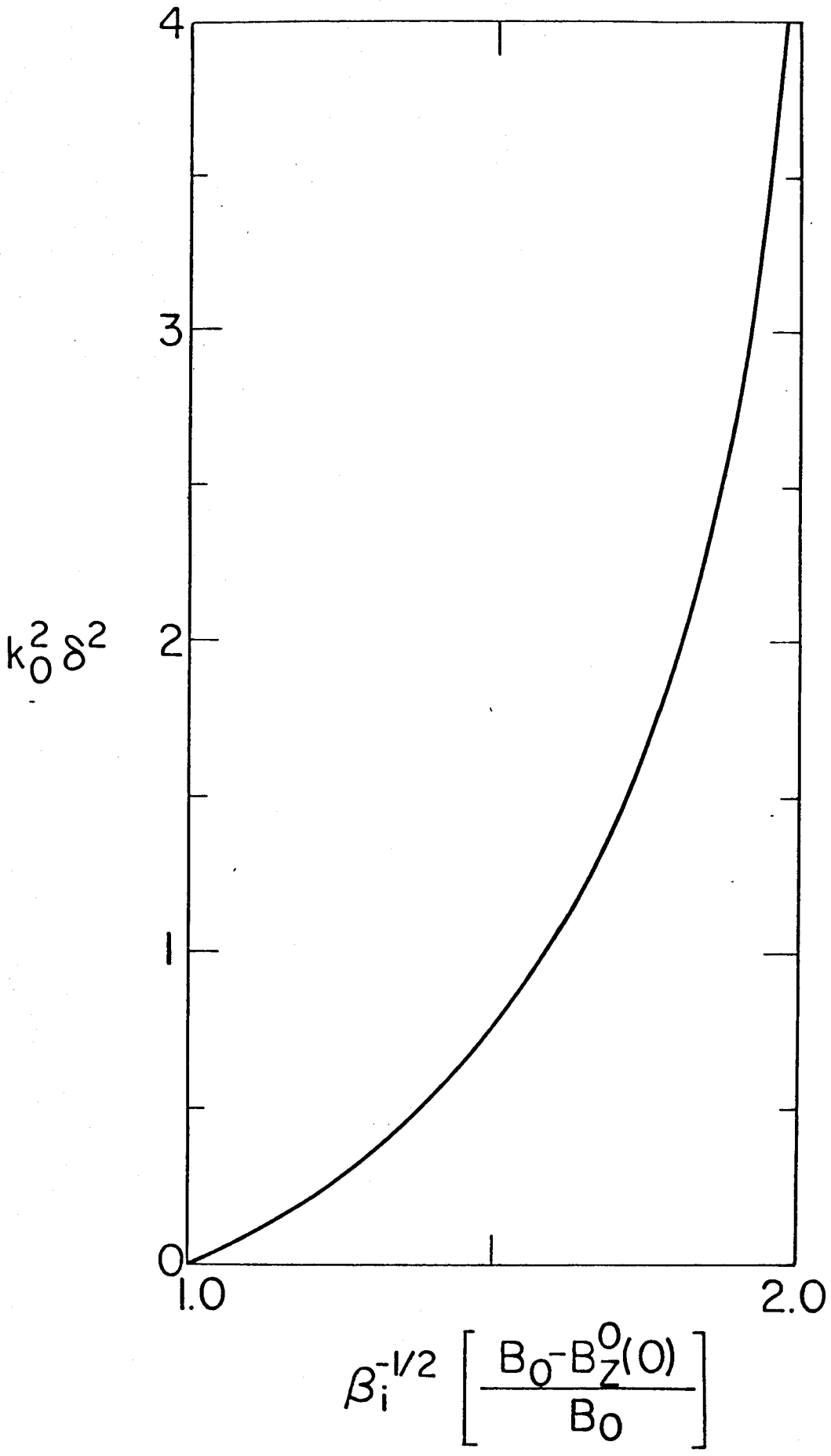

Figure 3.

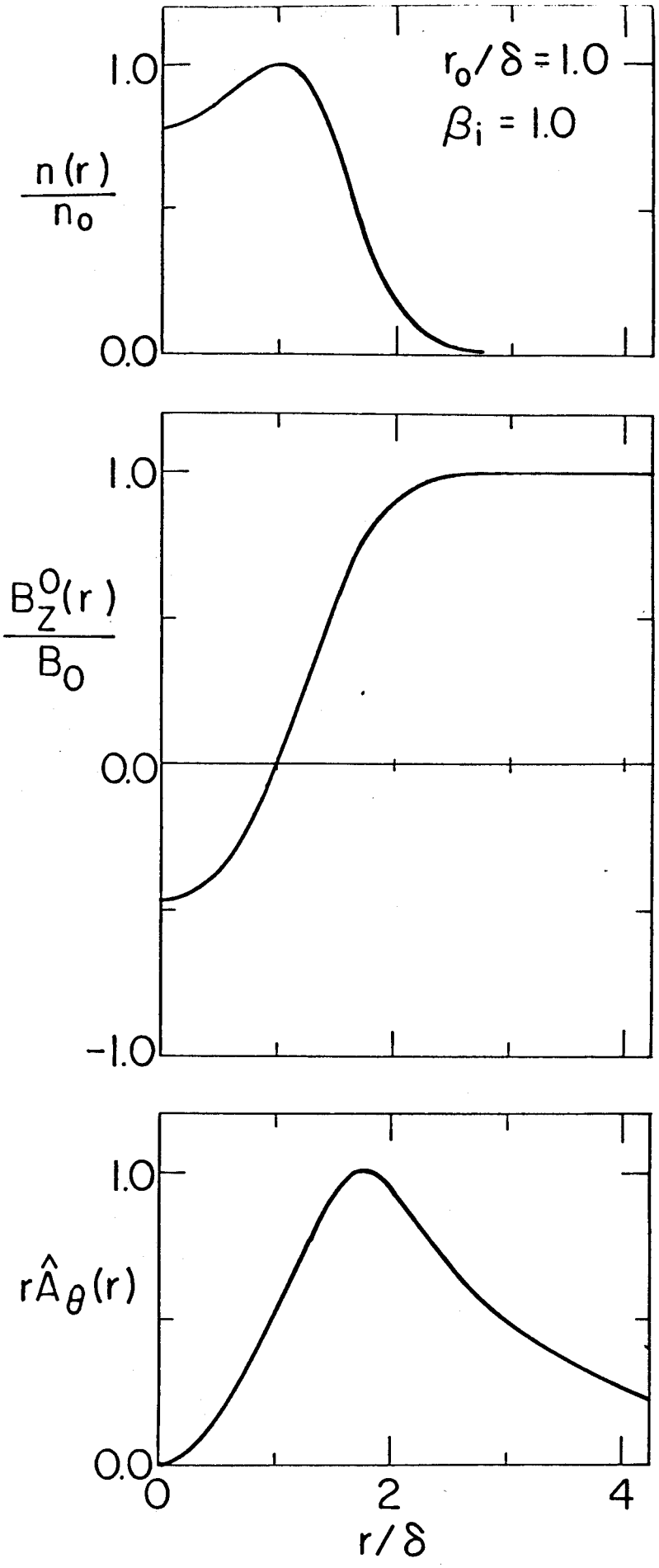
$r_0/\delta = 1.0$
$\beta_i = 1.0$
$\frac{n(r)}{n_0}$
1.0
0.0
$\frac{B_z^0(r)}{B_0}$
1.0
0.0
-1.0
$r\hat{A}_\theta(r)$
1.0
0.0
0
2
4
r/δ

Figure 4.

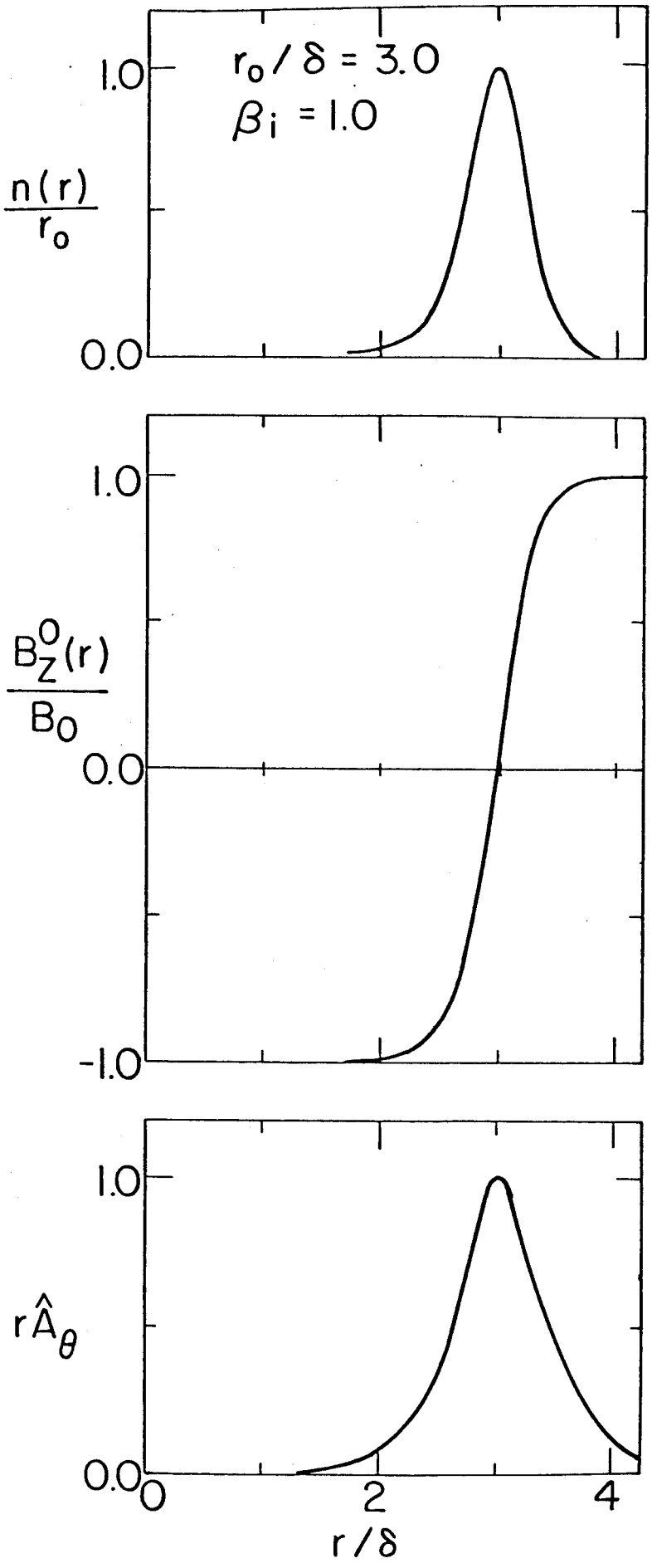
$r_o/\delta = 3.0$
$\beta_i = 1.0$
$\frac{n(r)}{r_o}$
1.0
0.0
$\frac{B_z^0(r)}{B_0}$
1.0
0.0
-1.0
$r\hat{A}_\theta$
1.0
0.0
0
2
4
r/δ

Figure 5.

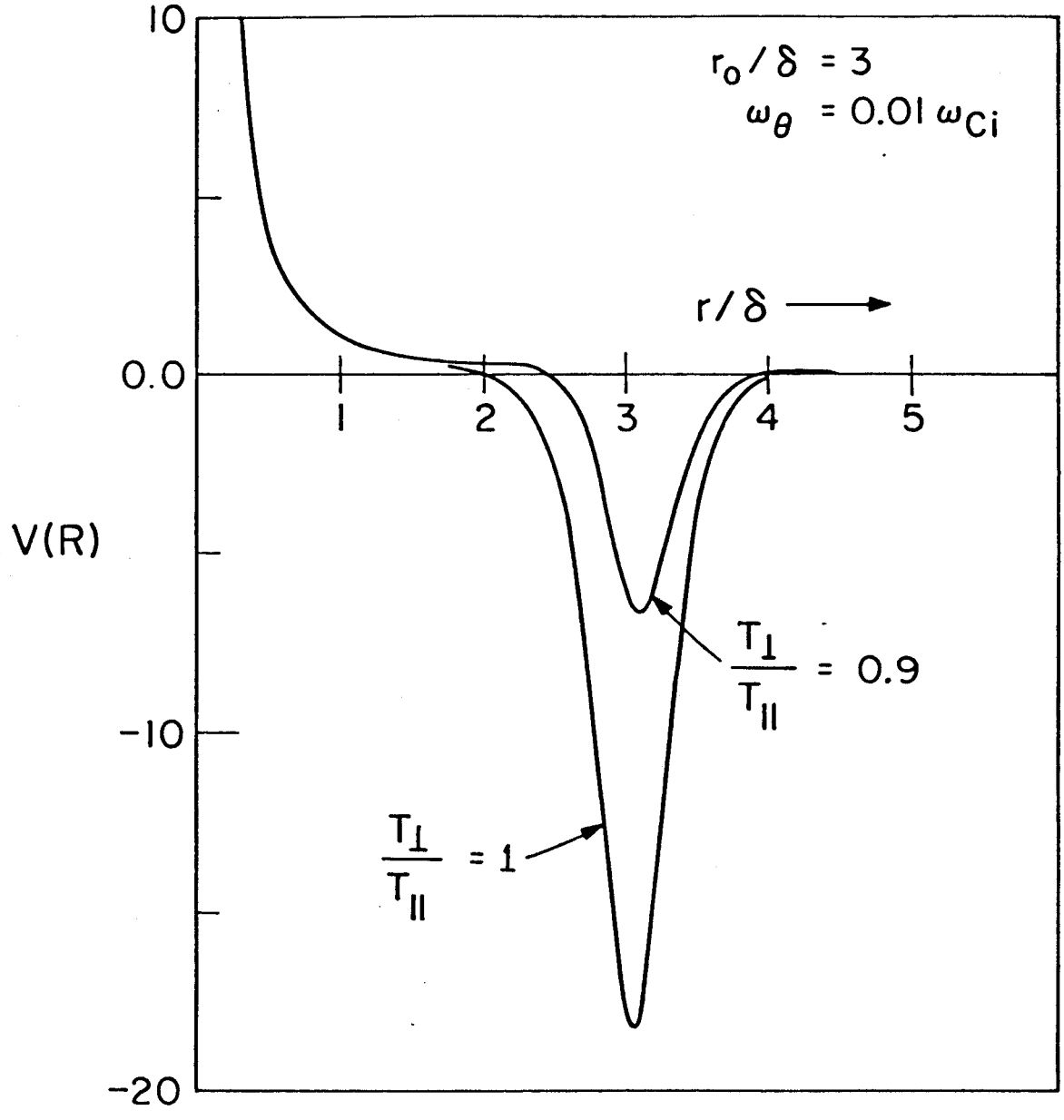
10
0.0
-10
-20
V(R)
1
2
3
4
5
$r_o/\delta = 3$
$\omega_\theta = 0.01\,\omega_{Ci}$
$r/\delta \longrightarrow$
$\frac{T_\perp}{T_{||}} = 0.9$
$\frac{T_\perp}{T_{||}} = 1$

Figure 6.

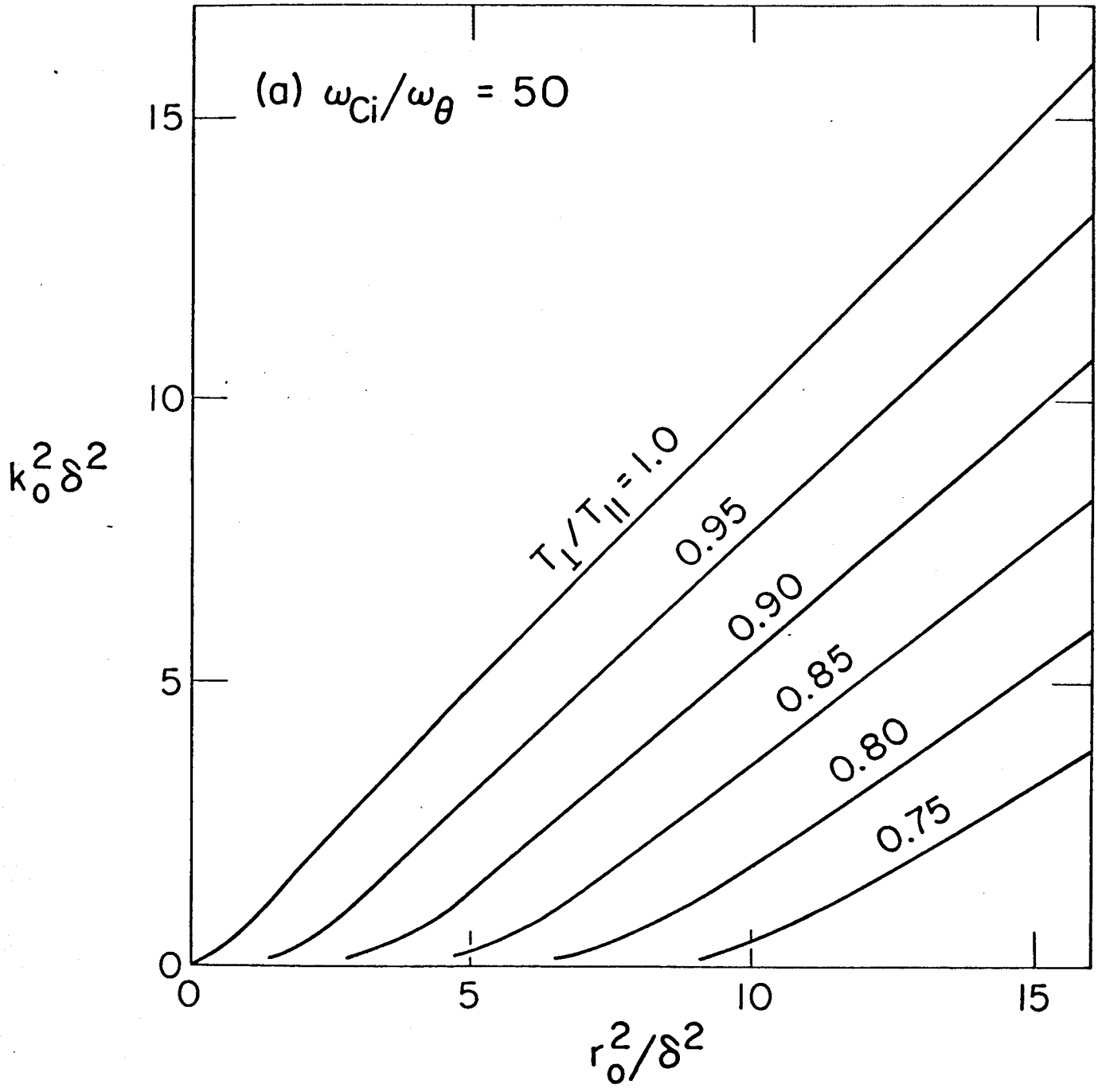
(a) $\omega_{Ci}/\omega_\theta = 50$
15
10
5
0
0
5
10
15
$k_0^2\delta^2$
r_0^2/δ^2
$T_\perp/T_{||}$=1.0
0.95
0.90
0.85
0.80
0.75

Figure 7.

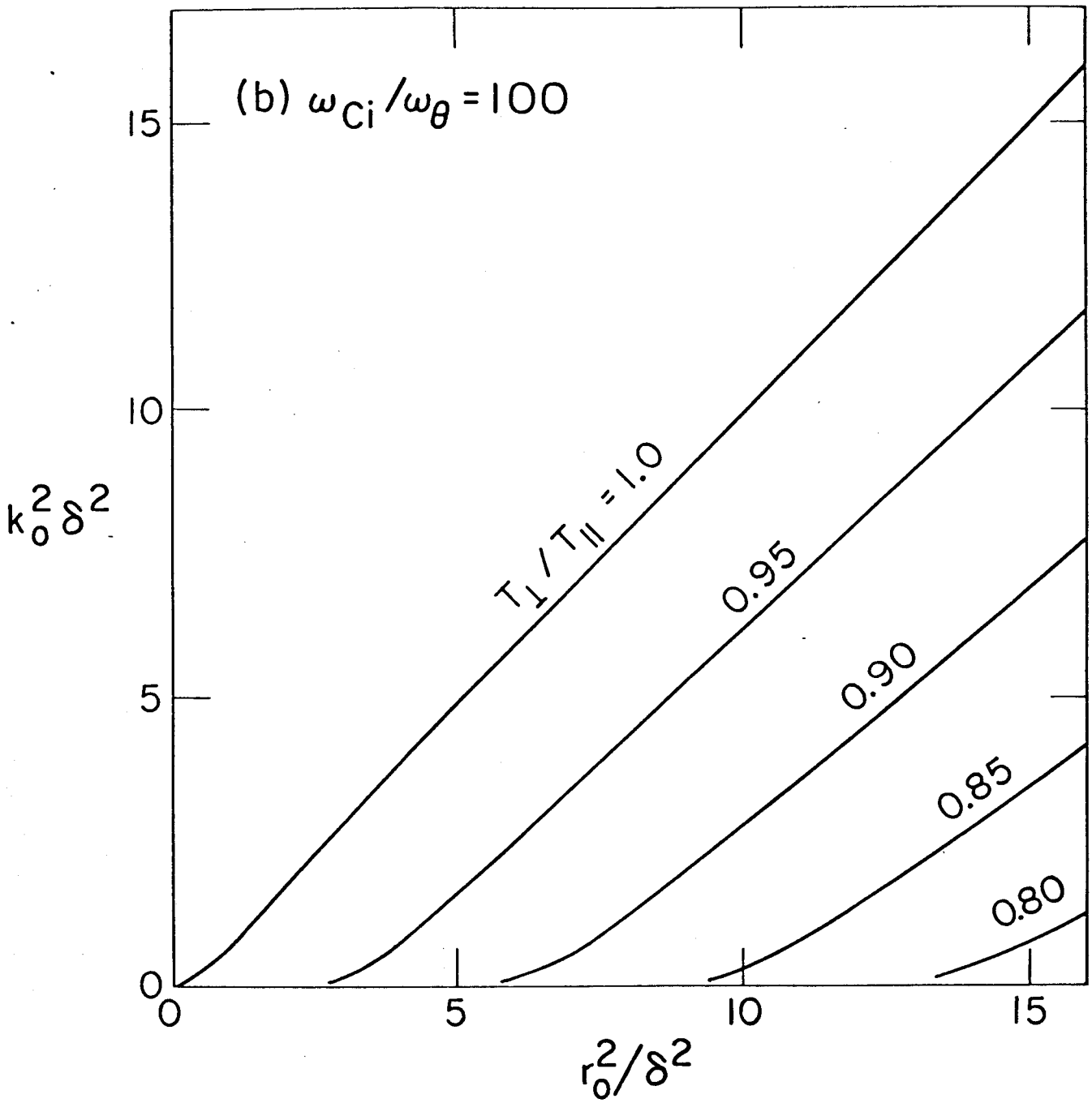
(b) $\omega_{Ci}/\omega_\theta = 100$
$k_0^2\delta^2$
r_0^2/δ^2
$T_\perp/T_{||} = 1.0$
0.95
0.90
0.85
0.80
0
5
10
15

Figure 8.

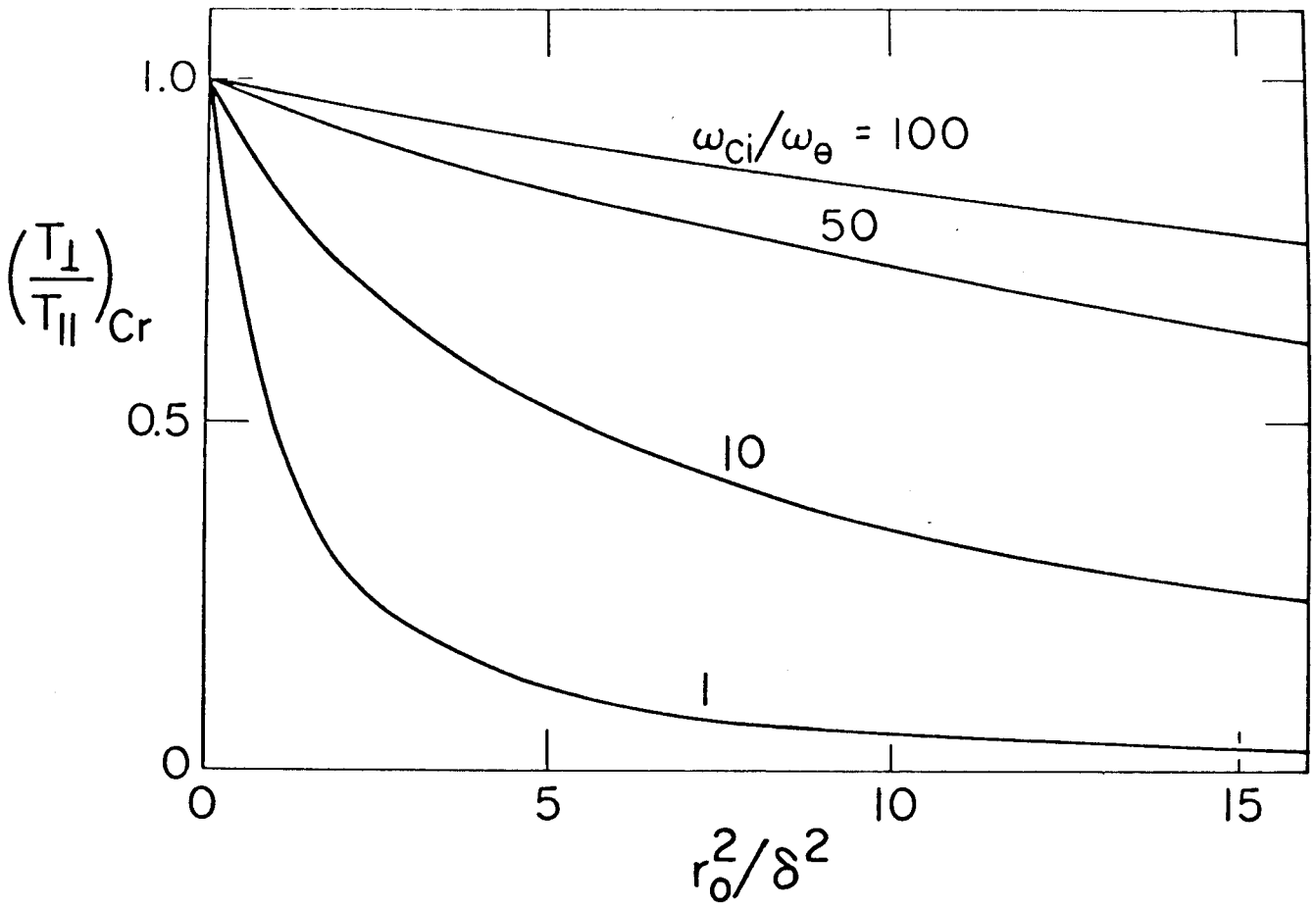
1.0
0.5
0
0
5
10
15
$\left(\frac{T_\perp}{T_\parallel}\right)_{Cr}$
r_o^2/δ^2
$\omega_{Ci}/\omega_\theta$ = 100
50
10
1

Figure 9.

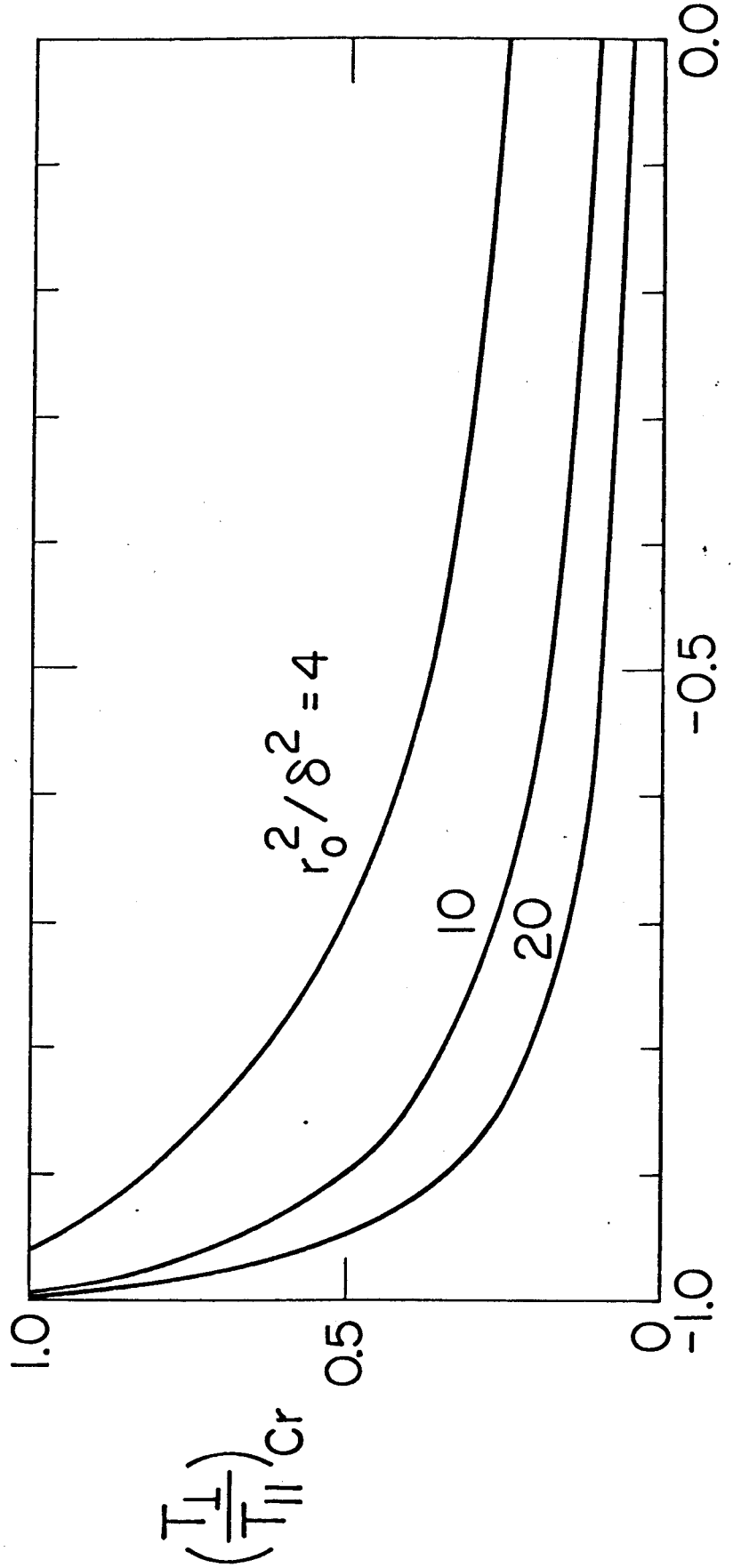
1.0
0.5
0
-1.0
0.0
-0.5
$\left(\frac{T_\perp}{T_{||}}\right)_{Cr}$
$B_z(0)/B_o$
$r_o^2/\delta^2 = 4$
10
20

Figure 10.

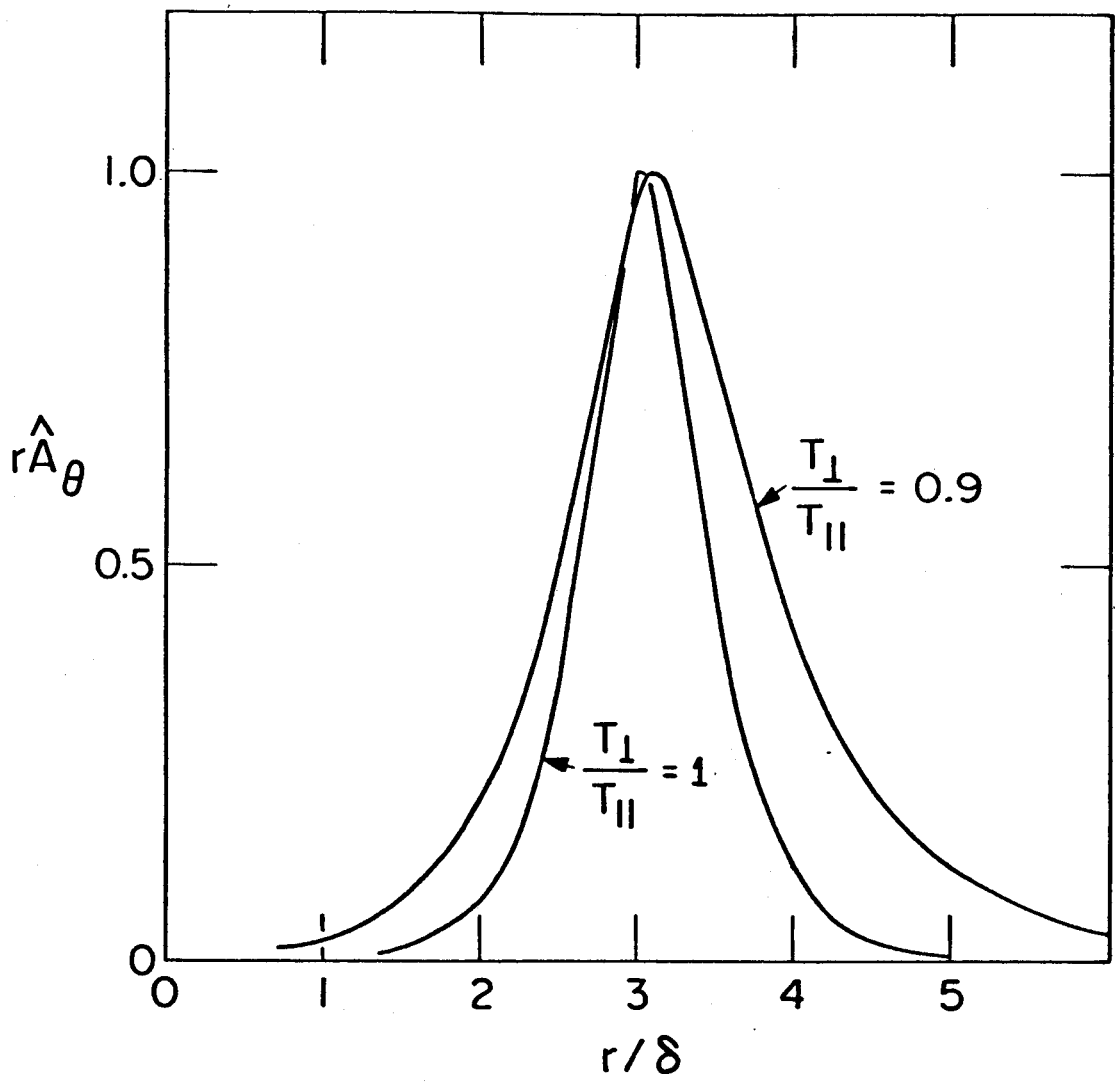
1.0
0.5
0
0
1
2
3
4
5
$r\hat{A}_\theta$
r/δ
$\frac{T_\perp}{T_{II}} = 0.9$
$\frac{T_\perp}{T_{II}} = 1$

Figure 11.